16th ICAAR LISBOA 2020-2022

16th International Conference on
Alkali-Aggregate Reaction in Concrete
Lisboa | LNEC | Portugal | 31 May - 2 June 2022

http://icaar2020-2022.lnec.pt

Studies on flexural behavior of post-tensioned concrete beam structure deteriorated by alkali-silica reaction

Takuro Maeda [(1)], Yukio Hiroi [(2)], Hideki Manabe [(3)], Takashi Yamamoto [(4)], Toyo Miyagawa [(5)]

(1) Engineering Department, CORE Institute of Technology Corporation, Osaka, JAPAN, t.maeda@coreit.co.jp

(2) Engineering Department, PC Division, IHI Construction Service Co., Ltd., Tokyo, JAPAN, yukio_hiroi@iik.ihi.co.jp

(3) CORE Institute of Technology Corporation, Osaka, JAPAN, manabe@coreit.co.jp

(4) Kyoto University, Kyoto, JAPAN, yamamoto.takashi.6u@kyoto-u.ac.jp

(5) Infra-System Management Research Unit, Kyoto University, Kyoto, JAPAN, miyagawa.toyoaki.6z@kyoto-u.ac.jp

Abstract

Alkali Aggregate Reaction (ASR) has been recognised as one of factors to degrade the mechanical properties of concrete structures. In this study, the purpose of this research mainly is looking for a proper quantitative approach to evaluate the degree of flexural capacity on ASR deteriorated structures. However, the internal condition of concrete members to be taken to observe deterioration into concrete structures are often inaccessible. Due to this limitation, the deteriorated levels and quantitative evaluation for flexural capacity on concrete structures still remain unknown. Therefore, an appropriate evaluation method to quantify the deteriorated levels and flexural capacity of concrete structures under ASR effect is significant undertaking. In this study, the authors proposed an analytical model to evaluate the flexural capacity of prestressed concrete (PC) beam deteriorated by ASR associated with measurement results, loading condition, and the crack density, as well as reactivity parameters related to mechanical properties, so that the degradation of concrete structures can be modelled for ASR conditions.

Keywords: *alkali aggregate reaction; crack density; expansion, prestressed concrete*

1. INTRODUCTION

Despite the fact that ASR has been considered as one of factors to cause decreased mechanical properties in structures, due to the limited information, it is unclear to define how such phenomenon affects the flexural capacity in existing ASR-affected PC beam structures. In addition, an appropriate method for quantifying the magnitude of flexural capacity after ASR damage occurred and initiated corrosion of embedded steel reinforcements still remain unknown. The primary objective of this study is to develop a reasonable method to estimate mechanical properties of ASR deteriorated concrete structures by estimating the crack density of concrete members or components' surface and the mechanical properties of drilled cores, and the performance of flexural capacity is then proposed. Based on this process, the correlation between decreased mechanical properties of concrete and flexural capacity of PC structures can be clarified.

The amount of expansion commonly serves as an index to describe the degree of ASR deterioration in concrete structures. However, the internal condition of concrete members to be taken to observe deterioration into concrete structures are often inaccessible. Moreover, for PC structures, in most common procedure for obtaining a core drilled from a concrete specimen, it is typically taken perpendicular to a horizontal surface. It is difficult to drill a core specimen from a longitudinal axis that prestressed tendons originally placed. Thus, to find more efficient approaches to examine the influence of ASR deterioration, the author proposed the method to quantify the mechanical properties of ASR deteriorated concrete at bridge axial direction by linking with the crack density of concrete members surface and the mechanical properties of drilled cores. Finally, the determination of input values associated with investigations and measurements discussed in this study on the effect of ASR were organized in simulations as detailed below.

2. DETERMINATION OF ASR DETERIORATED INDEX AND INPUT VALUES

2.1 Crack density and retention rate of mechanical properties

2.1.1 Amount of expansion and retention rate of mechanical property

The relationship between amount of expansion and retention rate of mechanical property can be seen in Figure 2.1 [1,2], in terms of elastic modulus (E_c), compressive strength (f'_c) and tensile strength (ft), respectively. In this figure, the data were obtained in the minimum limits for expansion in unconfined free-expansive specimens and retention rate of mechanical properties in unconfined cylindrical specimens. Linear regression analysis was applied to quantify the relationship between expansion and retention rate of mechanical properties for E_c. The scatter plot is presented in Figure 2.2. Due to difficulties in evaluating ASR-induced expansion on real structures during construction period, the measurements of crack density and retention rate of mechanical property in monitoring long-term exposed specimens were selected for assessing deteriorated index instead of the use of expansion amount on structures.

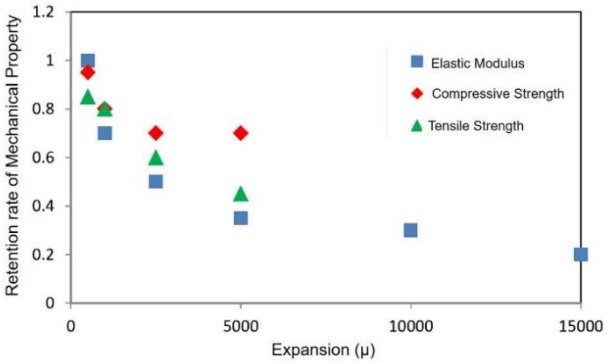

Figure 2.1 Expansion and retention rate of mechanical property relationship [1,2]

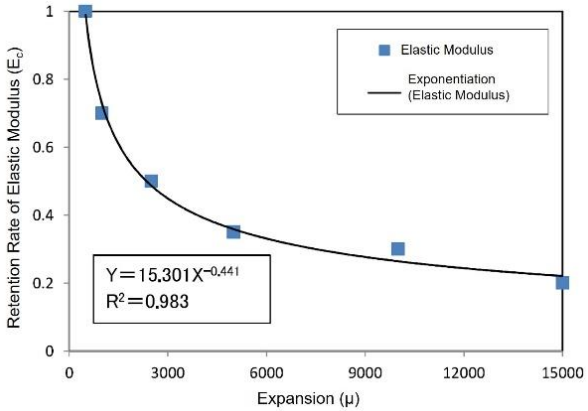

Figure 2.2 Expansion and retention rate of elastic modulus relationship

2.1.2 Crack density and amount of expansion

A series of measurements was conducted on both large scale and medium scale specimens to evaluate the values of crack density and expansion, where the values of expansion here are perpendicular to the direction of maximum expansion. In the case of PC structures, because the development of expansion is restrained by PC tendons and prestressing bars, etc., the greater expansion occurs in the direction that is perpendicular to and vertical to prestressing are than to the axial direction. The computation of crack density corresponding to the real structures has two criteria. The values of top and bottom of specimens were excluded from consideration during the crack density calculations. On the other hands,

the values of side of specimens with the cracks which were equal to or greater than 0.2mm (w≧0.2mm) were considered to be carried out in calculation. Additionally, in the case of ASR deteriorated PC Beam structures, existing cracks have wider width of cracks compared with new cracks and thus, the crack density has a tendency to converge [3]. Therefore, to compute crack density, the width of cracks should be introduced for evaluating ASR deteriorated condition (Method B). The crack density of Method A(m/m2) is defined as the length of cracks per unit of area, whereas for Method B (mm・m/m^2), the crack density is defined as the length × width of cracks per unit of area. Figure 2.3 shows the relationship between crack density of Method A and expansion that that the formation of the cracks occurred on side of specimens. Similarly, Figure 2.4 illustrates the crack density of Method B and expansion relationship that the formation of the cracks occurred on side of specimens. Compared with the results of Figure 2.3 and Figure 2.4, it is clear that Method B, introducing width of cracks into crack density computation, has a more significant correlation (R^2=0.931) than Method A. Therefore, in this study, to meet the aim of safety assessment, the Method B is adopted for determining crack density to evaluate the influence of expansion on ASR deteriorated PC specimens.

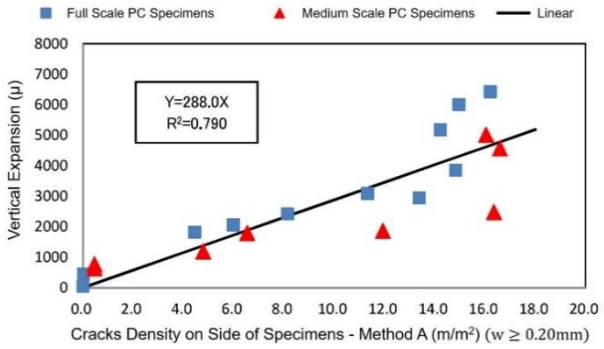

Figure 2.3 Relationship between vertical expansion and crack density on side of specimens-method A

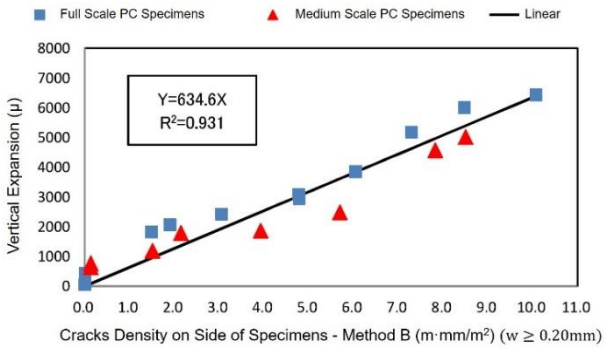

Figure 2.4 Relationship between vertical expansion and crack density on side of specimens-method B

2.1.3 Crack density and retention rate of mechanical property

To evaluate the relationship between crack density and retention rate of mechanical property on ASR deteriorated specimens, it was assumed that vertical expansion is equal to the expansion. As shown in Figure 2.4, linear regression equation (Y=634.6X) was applied to quantify the relationship between expansion at vertical direction and crack density of Method B on side of specimens. The equation was replaced vertical expansion with crack density of Method B, in writing a formula for linear regression line. Then the relationship between crack density of Method B and retention rate of mechanical property can be confirmed with the following equation:

$$\text{Crack density of Method B} = \frac{\text{Expansion}}{634.6} \quad (1)$$

2.2 Assessment of anisotropy difference in drilled cores and restrained of prestressing direction

2.2.1 Significance of mechanical properties of drilled cores under long- term exposure to ASR condition

A series of loading tests were conducted on ASR deteriorated specimens to assess the mechanical properties of drilled cores. Here, large scale specimens were assumed to be representative of actual in-situ condition. The tested pieces (TP) were obtained from the specimens after loading tests at axial and vertical direction. The locations of cores were plotted corresponding to inner and surface shown in Figure 2.5(1) and Figure 2.5(2), and the test results are summary in Figure 2.6.

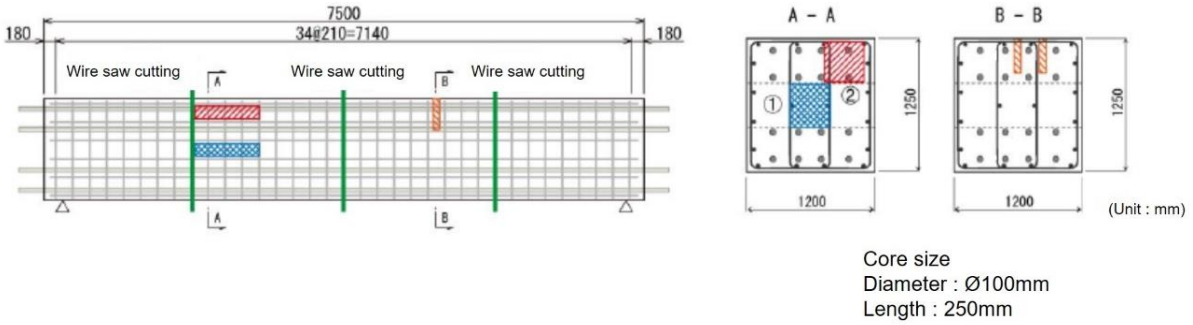

Figure 2.5 Location of drilled cores (TP)

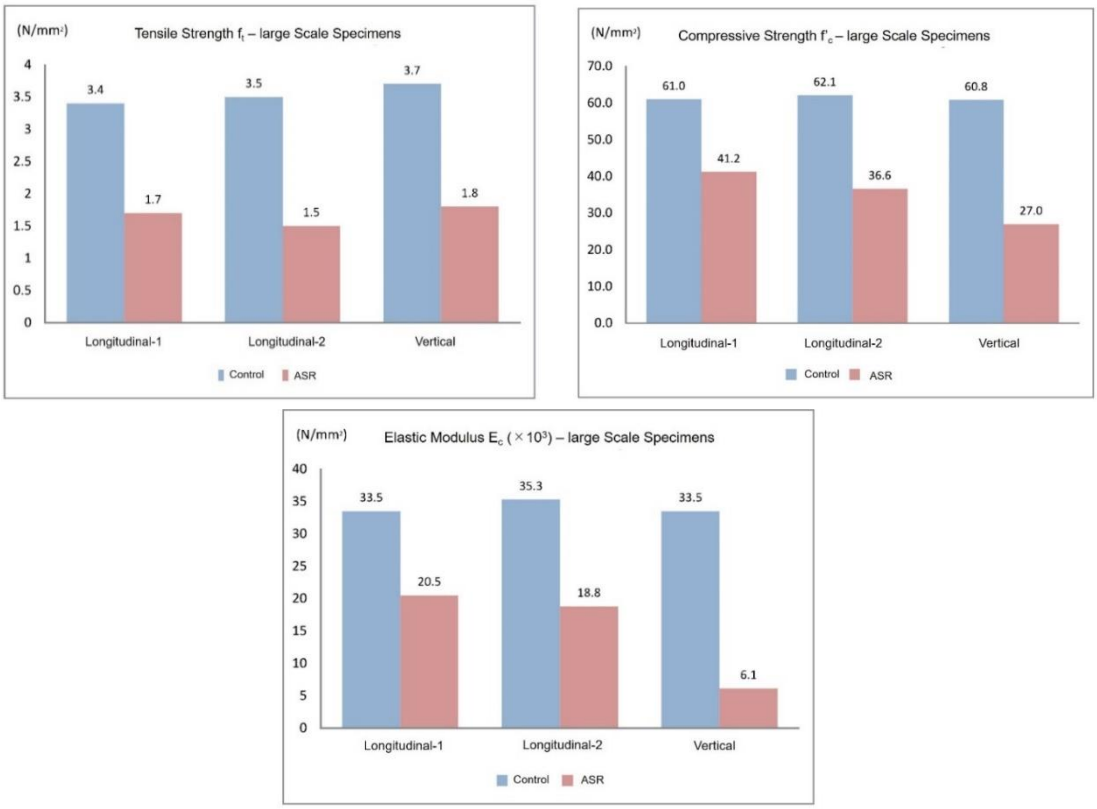

Figure 2.6 Summary of the mechanical properties of TP

2.2.2 Conversion coefficient determination at axial direction

In most common procedure for obtaining a drilled core drilled from a concrete specimen, a core specimen taken perpendicular to a longitudinal surface, so that its axis is perpendicular to the prestressing tendons as originally placed. In order to obtain the mechanical properties for real

applications, determination of conversion factors is needed. Nevertheless, one of key problems for the conversion is that the conversion coefficient may yield significantly with characteristics of existing structures, the levels of ASR deterioration and mechanical properties. Hence, an appropriate conversion coefficient for core specimens is difficult to determine.

Currently, it is noted that the drilled cores perpendicular to prestressing are applied to evaluate flexural capacity in most cases. Previous studies [4-11] have investigated reduction rate of compressive strength (f'_c) and elastic modulus (E_c) on TP of ASR deteriorated PC beam structures. The obtained data is summary in the Table 2.1 and presented in Figure 2.7 and Figure 2.8.

In this study, a major modification of the input parameters for TP's mechanical properties has to be replaced measurement values to reduction rate B, where reduction rate B is the value in perpendicular direction to the axial direction (the values in perpendicular direction / the values in axial direction). The reduction rate B corresponding to f'_c and E_c at axial direction are listed in Table 2.1 and shown on Figures 2.9 and Figure 2.10.

In the case of f'_c at axial direction, the reduction rate B is in the range of 43% to 96%, and the average of which is about 71%. Whereas, the reduction rate B of Es falls into the range of 30%~85%, tending to have averagely decreased by 58 %. Here, conversion coefficient (α) in axial direction defines as an inverse relationship to the reduction rate B, and then the new value at axial direction can be computed from multiplication by α and TP values corresponding to perpendicular and vertical direction, respectively. However, the magnitude of reduction rate B is dependent on α. It was inferred that the selection of large value in reduction rate B (i.e 43% [11]) lead to have large value in α. On the other hand, for the selection of low reduction rate of B might overestimate the design values.

Consequently, to obtain the TP values of ASR deteriorated PC beam structures, a unique set of conversion coefficient at axial direction, namely, α_1=1.4(100/71) and α_2=1.7(100/58) were determined in this study. In the case of tensile strength (f_t), the scatter plot had insufficient data points to perform the analysis. Thus, based on author's research [10] (Figure 2.11), f_t = 1/24 f'c for the input setting.

Table 2.1 Conversion coefficients on compressive strength and elastic modulus

	Type of structures		Core		Compressive strength				Elastic Modulus			
	PC/ RC	Structures	Direction	Size	Design	Measurement	Reduction rate A	Reduction rate B	Design	Measurement	Reduction rate A	Reduction rate B
					a	b	b/a	Axial direction	c	d	d/c	Axial direction
				mm	N/mm²	N/mm²	%	%	N/mm²	N/mm²	%	%
Ueda et al	PC	Post tensioned specimen	Axial	Ø100×200	36.0	48.0	133		29800	32300	108	
			Axial		36.0	40.3	112	96	29800	21000	70	
			Vertical		36.0	46.1	128	88	29800	27500	92	85
			Vertical		36.0	42.2	117		29800	19400	65	60
Tomiyama et al	PC	Prestressed H	Perpendicular	Ø68 × 100	49.3	44.3	90		33000	15200	46	
Kawashima et al	PC	PC beam	Perpendicular to the axis of bridge footing	Ø68 × 130	35.0	37.9	108		27800	12000	43	
					35.0	44.4	127		27800	19500	70	
Inagaki et al	PC	Post tensioned specimen	axis of bridge	Ø55 × 110	50.0	48.0	96		33000	20500	62	
			Vertical		50.0	40.0	80	83	33000	16500	50	80
			Perpendicular		50.0	37.0	74	77	33000	14000	42	68
Aikyo et al	PC	Prestressed H	Perpendicular		50.0	30.0	60		33000	6500	20	
Minato et al	PC	Post tensioned T	Perpendicular		40.0	40.0	100		31000	23200	75	
	PC	Post tensioned T	Perpendicular		40.0	40.0	100		31000	14000	45	
	PC	Post tensioned T	Perpendicular		40.0	35.0	88		31000	7800	25	
	PC	Prestressed H	Perpendicular		50.0	55.0	110		33000	24750	75	
Author	PC	Post tensioning specimen	Inner of bridge axis	Ø100 × 250	36.0	41.2	114		29800	20500	69	
			Surface of bridge axis		36.0	36.6	102		29800	18800	63	
			Vertical		36.0	27.0	75	66	29800	6100	20	30
Report of Hansin Express Co, Ltd.	PC	PC specimen	Axial	Ø75 × 150	36.0	40.2	112		29800	21900	73	
			Perpendicular		36.0	27.1	75	67	29800	16000	54	73
			Perpendicular		36.0	20.5	57	51	29800	7200	24	33
			Vertical		36.0	17.2	48	43	29800	6700	22	31

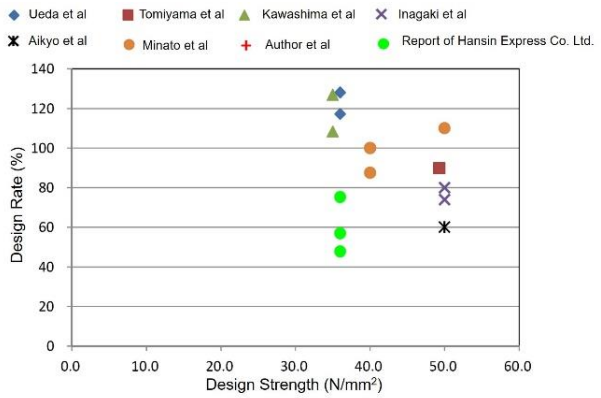

Figure 2.7 Reduction rate of compressive strength (vertical direction along bridge axis)

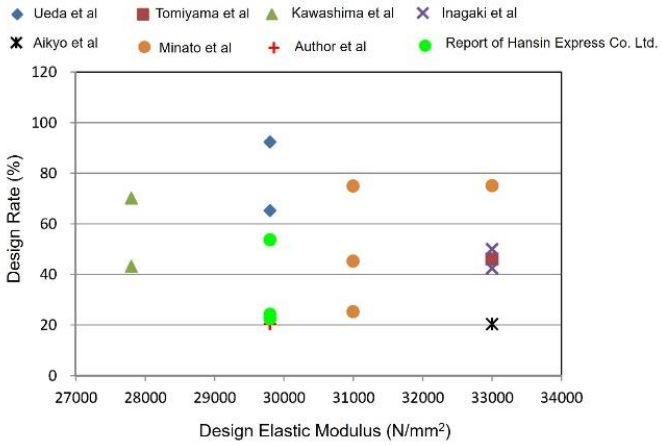

Figure 2.8 Reduction rate of elastic modulus (vertical direction along bridge axis)

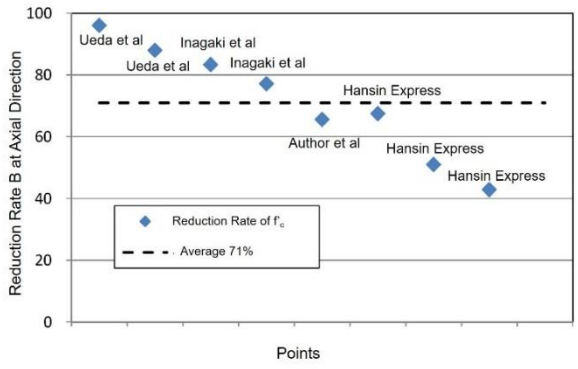

Figure 2.9 Reduction rate of compressive strength

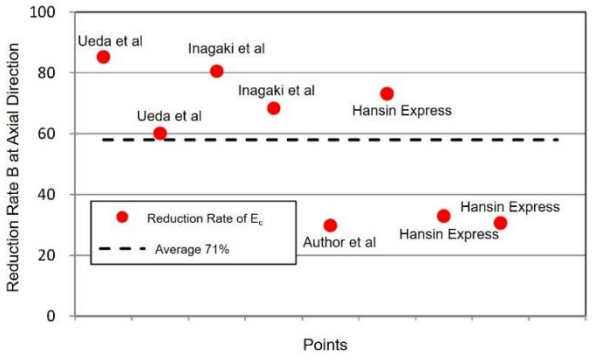

Figure 2.10 Reduction rate of elastic modulus

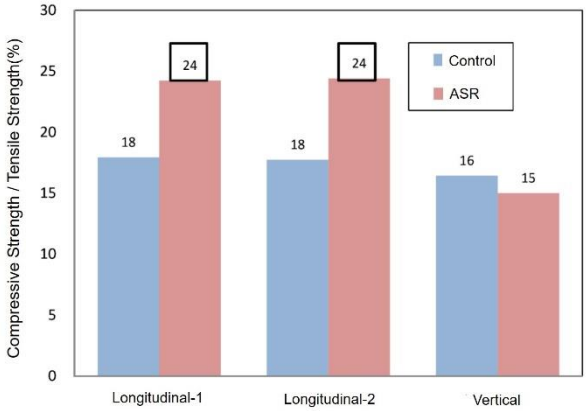

Figure 2.11 compressive strength / tensile strength (%)

3. FLEXURAL STRENGTH OF PC BEAM SPECIMENS ASSESSED BY DETERIORATED INDEX

3.1 Flexural capacity verification via crack density method

3.1.1 Crack density Evaluation based on Method A and Method B

Recently study revealed that the formation of the cracks occurred in PC structures inhibit the tendency of the cracks to stop propagation. The concept of Method B which has been discussed above was introduced by considering the width of cracks and expansion to evaluate the condition of ASR deteriorated structures. However, in most of cases, Method A is commonly used to describe the crack density of ASR deteriorated condition. In the following research, Method B was applied to quantify and examine crack density based on the results obtained from Method A. The results of Method A and Method B are shown in Figure 3.1.

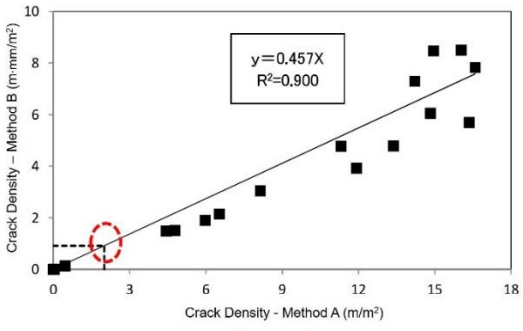

Figure 3.1 Method A and Method B relationship

3.1.2 Crack density estimation at axial direction based on Method B

Experimental studies on mechanical properties of concrete specimens under large scale tests were conducted and summarized in Table 3.1. The modelling simulation employed for this study to estimate flexural capacity is schematically shown in Figure 3.2.

The estimation for crack density of Method B (E_B) can be computed numerically by crack density of method B on side of specimens, in which is 10.078m・mm/m² (W≧0.2mm) at concrete age of 2718 days. The values of E_B can be computed from expansion and retention rate of mechanical properties, which illustrated by Equation (2) to Equation (5), and multiplication by retention rate and soundness values. Equation (2) can be obtained with the regression analysis between expansion and crack density of Method B as shown in Figure 3.1. Moreover, Equation (3) ~Equation (5). which defined by the regression analysis of the crack density of Method B were plotted against corresponding retention rate of mechanical properties as presented in Figure 3.3~Figure 3.5, respectively.

$$\text{Expansion} \qquad Y = 6.34.6X \tag{2}$$

$$\text{Compressive strength} \qquad Y = 0.883X^{-0.134} \tag{3}$$

$$\text{Tensile strength} \qquad Y = 0.846X^{-0.281} \tag{4}$$

$$\text{Elastic Modulus} \qquad Y = 0.891X^{-0.441} \tag{5}$$

in which, X is crack density of Method B.

The computed results for retention rate of mechanical properties are listed in Table 3.2. The E_B for flexural capacity analysis in the study presented in Table 3.3, at which the ratio of average TP is obtained from the average value at axial 1 and axial 2 (Figure 2.6).

Table 3.1 Mechanical properties of tested specimens

	Soundness values (N/mm²)	ASR					
		Surface values (N/mm²)	Ratio of surface to soundness (%)	Internal values (N/mm²)	Ratio of internal to soundness (%)	Vertical values (N/mm²)	Ratio of vertical to soundness (%)
f'_c	61.6	36.6	59%	41.2	67%	27.0	44%
f_t	3.45	1.5	43%	1.70	49%	1.80	52%
E_c	34400	18800	55%	20500	60%	6100.0	18%

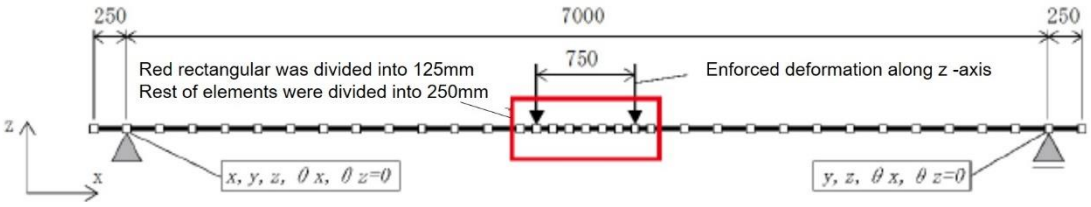

Figure 3.2 Schematic diagram of FEA modelling system

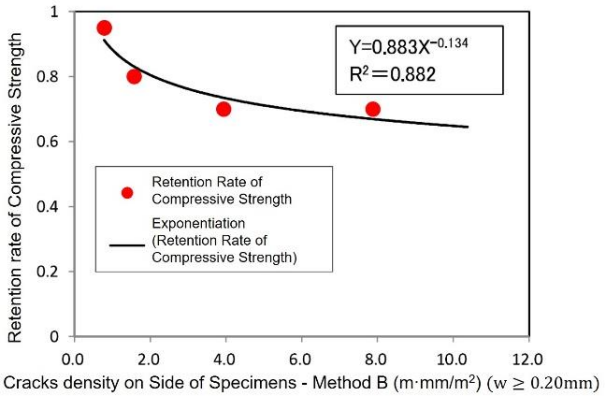

Figure 3.3 Crack density of Method B and compressive strength relationship

Table 3.2 Retention rate of mechanical properties

Crack density of Method B (X) (m・mm/m²)	Expansion (μ)	Equation		Crack density of Method B (X) (m・mm/m²)	Retention rate of compressive strength	Equation
10.078	6395	(5.4.1)		10.078	0.65	(5.4.2)
Crack density of Method B (X) (m・mm/m²)	Retention rate of tensile strength	Equation		Crack density of Method B (X) (m・mm/m²)	Retention rate of elastic modulus	Equation
10.078	0.44	(5.4.3)		10.078	0.32	(5.4.4)

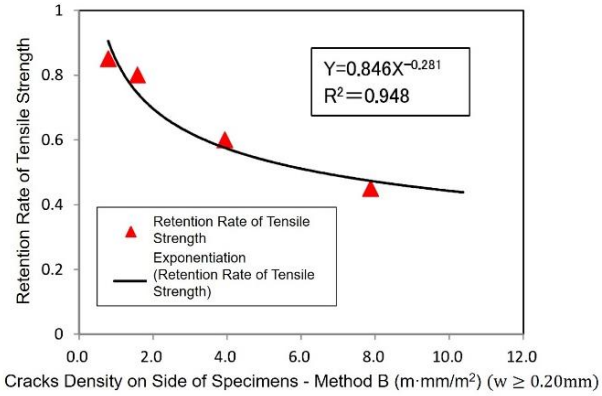

Figure 3.5 Crack density of Method B and elastic modulus relationship

Table 3.3 Results of Estimation B for flexural capacity analysis

	Retention rate of mechanical properties	Soundness value N/mm²	Estimation N/mm² ①	Average values at TP axis N/mm² ②	Ratio ①/②
Compressive strength f'_c	0.65	61.6	40.0	38.9	1.03
Tensile strength f_t	0.44	3.5	1.5	1.6	0.95
Elastic modulus E_c	0.32	34400	11060	19650	0.56

3.2 Flexural capacity verification via conversion coefficient at axial direction

As mentioned above, the observation indicated the existing difference between the constrained direction of prestressing and the orientation of drilled core. It doesn't render the true values of anisotropic mechanical properties for specimens. Such true mechanical properties at axial direction can be determined from multiplication by conversion coefficient along bridge axis and vertical TP values which is anisotropic to prestressing. Obtained results can be surface valued. A diagram of calculated area (hatched) is shown in Figure 3.6, and flexural capacity of large-scale PC beam was estimated by modelling system given in Figure 3.2, while the use of conversion coefficient at axial direct (E_A) to define the mechanical properties values for flexural capacity were listed in Table 3.4.

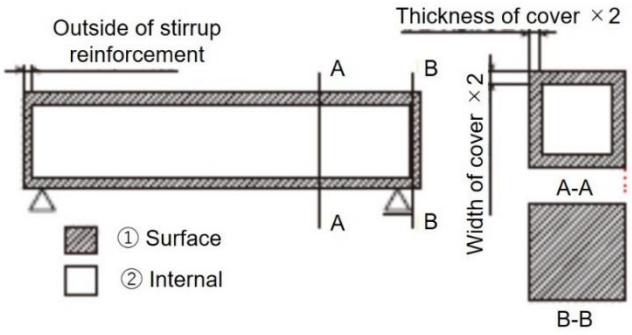

Figure 3.6 Diagram illustrating details of large -scale PC beam specimen

Table 3.4 Estimation of flexural capacity at axial direction

		Vertical Core values	Conversion coefficient at bridge axis	Estimated Mechanical property ①	Average values at TP axis ②	Ratio ①/②
f'_c	N/mm²	27.0	1.4	37.8	38.9	0.97
f_t	N/mm²	1.8	σc/24	1.6	1.6	0.98
E_c	kN/mm²	6.1	1.7	10.4	18.8	0.55

3.3 Comparison of various methods

The results of various methods were simulated by the proposed model with corresponding coefficient as shown in Table 3.5 and their respective data results are shown in Figure 3.7 and 3.8. The results of TP axis simulated by FEA modelling system are shown in Table 3.6 and Figure 3.9, in which the values of TP axial expressed in ratio are shown in Figure 3.7.

Table 3.5 Summary of simulated results on three methods

	No.	Loads as tensile – stress crack occurred (kN)	Max. Load (kN)	Displacement under load of 1000kN (mm)	Displacement under load of 2000kN (mm)
TP axis	1	1308	4628	1.43	3.05
Method B estimation	2	1374	4488	1.78	3.77
Axial estimation	3	1402	4450	1.81	3.84

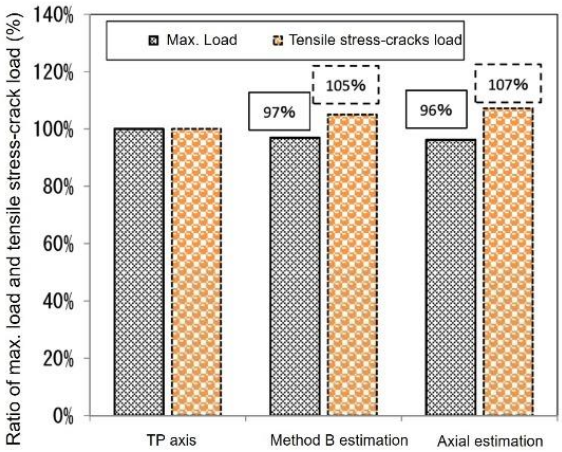

Figure 3.7 Comparison between max. load and tensile stress-crack load

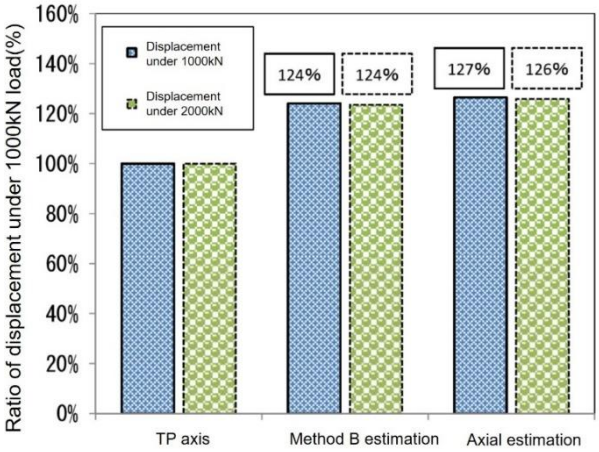

Figure 3.8 Displacement comparison under 1000kN and 2000kN load

Table 3.6 Comparison of Maximum Loads

Large scale soundness (kN)			Large scale ASR (kN)		
Measurements	Solid model	FEA model	Measurements	Solid model	FEA model
4908	4901	5090	4885	4611	4616
Ratio of Measurements	100%	104%	Ratio of Measurements	94%	94%

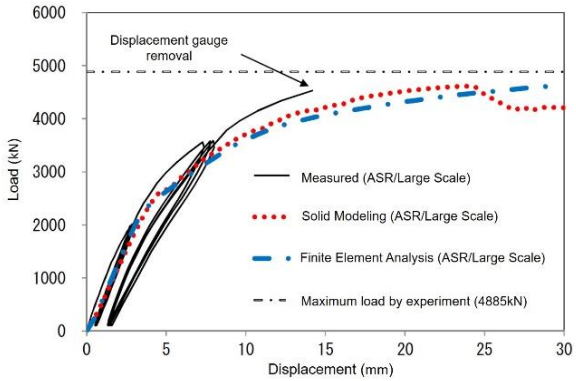

Figure 3.9 Comparison between model prediction and test results on ASR specimen

3.4 Summary of results

Regarding to the Maximum loads, by using the results of TP at axial direction (TP axis) as a comparison basis for ASR deteriorated specimens, both E_B and E_A reached 96% consistency for prediction. In the case of tensile stress-crack loads, model simulations were also compared with TP axial results. The predicted loads of E_B and E_A are 105% and 107%, respectively. These implied that both methods provided prominent accuracy compared with TP axial results. Therefore, either E_B or E_A can be selected for evaluating tensile loading during the initiation and evolution of a crack. Considering the displacement, a direct comparison of the difference in displacements by estimated methods is approximately 11mm, inferring that the two methods can be introduced for assessment. As a consequence, the findings concluded that crack density method B and conversion coefficient at axial direction can be selected for assessing flexural capacity on ASR deteriorated PC beam structures.

4. CONCLUSION

To examine the influence of ASR deterioration on concrete structures, estimation of mechanical properties of ASR deteriorated concrete specimens by crack density and mechanical properties of drilled cores were proposed. The input data, for instance, mechanical properties, and conversion coefficients,

which were introduced to simulate and assess flexural capacity of ASR deteriorated structures was efficient interpretation in this study. The main results and conclusions drawn from this study are summarized below.

(1) A FEA model accounting for the influence of ASR deteriorated concrete was performed. Using the set of determined input data proposed by authors, all comparisons between the experimental data and the numerical simulations demonstrated that the model can approximately simulate the initial stiffness and maximum load for PC beam structures.

(2) According to the results of long-term measurements, it is confirmed that crack density of method B was linked and correlated to expansion.

(3) It is clearly shown from those figures that expansion has relationship between retention rate of mechanical properties and crack density of Method B. Such relationship can be used to estimate retention rate of mechanical properties by crack density Method B.

(4) It is confirmed that either crack density of Method A or Method B is thought to be relatively reliable.

(5) To estimate the mechanical properties of ASR deteriorated structures on the constrained direction of prestressing, it can be determined from multiplication by conversion coefficient and mechanical properties of drilled cores.

5. REFERENCES

[1] Japan Society of Civil Engineers (2005) State-of-the-art report on the countermeasures for damage due to alkali-silica reaction – Rupture of reinforcing bars. Concrete Library (124). Japan

[2] CLARK, L.A. (1990) Structural aspects of alkali silica reaction. Structural Engineering Review, 2, pp 81-87

[3] Prestressed Concrete Contractors Association (2009) State-of-the-art report on the countermeasures for ASR. Japan

[4] Ueda N, Nakamura H, Kunieda M, Maeno H, Morishita N, and Asai H (2011) Evaluations on ASR damage of concrete structure and its structural performance. Journal of JSCE, E2(67.1), pp 28-47

[5] C Tomiyama J, Yamada K, Kaneda K, Iraha S, Oshiro T(2011) ASR diagnosis by petrographic and evaluation of mechanical performance of ASR deteriorated pretensioned PC Beam. Journal of JSCE, E2, vol.67, No.4, pp.578-595

[6] Kawashima K, Kousa K, Matsumoto S, Miura M (2011) Quantitative Evaluation of ASR deterioration Level based on survey result of existing structure. Journal of JSCE, E2, Vol.67, No.1, pp.103-120, 2011

[7] Inagaki T, Obana Y, Ishi T, Torii K (2009) Evaluation of mechanical properties of drilled cores on ASR deteriorated PC concrete beam structure. Concrete Journal, vol.31, No.1, pp.1237-1242

[8] Aikyo K (2007) Soundness assessment and investigation on ASR deteriorated PC bridge. Concrete Journal, vol.45, No.8, Page of concrete diagnosis engineer, pp 79-83

[9] Minato T, Ishii K, Ushiya S, Torii K (2011) Characteristics of cracks and current status of countermeasures for ASR deteriorated prestressed concrete bridge. Proceedings of the concrete structure scenarios, JSMS,11, pp 471-478

[10] Hiroi Y, Okubo T, Kirikawa K, Miyakawa T (2013) Experimental report on full scale ASR deteriorated PC specimens in loading test, Proceedings of the Symposium on Developments in Prestressed Concrete, 22nd, pp195-198

[11] Hanshin expressway management technology center (2008), Report of maintenance management methods for ASR-affected structures, Hanshin Expressway Co., Ltd., Japan

Studies on flexural behavior of post-tensioned concrete beam structure deteriorated by alkali-silica reaction
Takuro Maeda; Yukio Hiroi; Hideki Manabe; Takashi Yamamoto; Toyo Miyagawa